Original Study   **Open Access**

Imad Kadiri*, Younès Tahir, Omar Iken, Saïf ed-Dîn Fertahi, Rachid Agounoun

Experimental and statistical analysis of blast-induced ground vibrations (*BIGV*) prediction in Senegal's quarry

Abstract: Extractive industries often use explosives to destroy rocks, and productivity requirements tend to increase the charges of the explosives. The blasts induce vibrations, which result in a potential damage of the surrounding structures. Therefore, the prediction of vibrations should be described with accuracy, in order to ensure the safety of engineered structures. However, the prediction of vibrations' levels remain a complicated issue, because it involves numerous parameters correlated to the quarry site.

In this paper, statistical analysis based on the peak particle velocity *(PPV)* and the attenuation law has been carried out to assess the safety charges (Q) for different distances (R) between the blast and the considered structure to secure. Moreover, the experimental investigations were conducted on the quarry site of *"Sococim"*, which is located on the south coast of Senegal. To ensure the safety of the *"Conveyor belt"* and *"Panel 1 (Upper exploitation level)"* sites, the *PPV* should be less than 10 mm/s. In fact, the attenuation model has been used to assess the safe charge weights of the explosive (Q) to be used at the *"Conveyor belt"* site and at the *"Panel 1 (Upper exploitation level)"* site. Therefore, the safe charge weights per delay (Q) were respectively 116 kg and 13.75 kg.
Keywords: *BIGV, PPV*, attenuation law, blast, charge per delay, statistical analysis, safety.

*Corresponding author: Imad Kadiri,** Université Moulay Ismail (UMI), Laboratoire d'Etude des Matériaux Avancés et Applications (LEM2A), Ecole Supérieure de Technologie de Meknès, Km 5, route d'Agouray, N6, 50040, Morocco, E-mail: imad _ kadiri@hotmail.com
Younès Tahir, Omar Iken, Rachid Agounoun, Université Moulay Ismail (UMI), Laboratoire d'Etude des Matériaux Avancés et Applications (LEM2A), Ecole Supérieure de Technologie de Meknès, Km 5, route d'Agouray, N6, 50040, Morocco
Saïf ed-Dîn Fertahi, Université Sidi Mohamed Ben Abdellah (USMBA), Ecole Supérieure de Technologie de Fès, Route d'Imouzzer BP, 2427, Morocco

Nomenclature

B	
f	Empirical factors
k	
n	
m	
Q	charge per delay (kg)
R	distance (m)
VL	longitudinal velocity (m/s)
VT	transversal velocity (m/s)
VV	vertical velocity (m/s)
WB	overall charge weight (kg)

Abbreviations

ANN	Artificial Neural Network
TB	Trial Blast
BIGV	Blast Induced Ground Vibration
FEM	Finite Element Method
FFT	Fast Fourier Transform
PPV	Peak Particle Velocity
SD	Scaled Distance
SM	Statistical Modelling

Superscripts

α	
b	Empirical factors
β	
γ	
λ	

1 Introduction

1.1 Background of the research

Explosives are used in most large-scale development projects such as high-speed lines, highway projects and hydroelectric development as an energy source to destroy rocks and concretes.[1] Several technics can be used to

enhance the productivity of the operated site, for instance, by increasing the diameters of the borehole, by adjusting the total charge or by controlling the charge per delay. [2] Actually, it is difficult to control the explosive energy involved in mine blasting, which can be considered as the main source of disturbance described by the induced vibrations, noises and projections of rock fragments.[3] In this paper, an experimental study was carried out on the site of *"Sococim"*, to evaluate the critical load of the explosive (Q) to be used, in order to avoid the adverse effects of blasting, while keeping an accurate level of productivity.

1.2 State of the art of blast induced ground vibration (BIGV) studies

In the recent years, the sensitivity of populations to the environment has increased. The urbanization around the exploitation sites has intensified, and both of the comfort and safety threshold are required to decrease the damage level such as noises, projections of rock fragments and vibrations induced by the exploitation of quarries. In fact, the threshold comfort of human's sensitivity is twenty times lower than the threshold criteria, which is commonly used to limit the damage of structures.[4]

When the explosion occurs, 5 to 10% of the energy propagates as an over-pressure in the air, without affection, the building's structures except on glazed facades,[5] while 10 to 20% of the energy propagates as a vibration in both fluids and solids parts of the ground. It is noted that the wave propagates in an elastic medium as an earthquake at different velocities, depending on its type (longitudinal, transversal or surface wave) and the elastic properties of the medium. The remaining energy part is used to destroy the rocks.

BIGV are largely quantified in terms of *PPV* and its associated frequency. The intensity of ground vibrations depends on various parameters, which can be defined as controllable and uncontrollable parameters.[6] For instance, the controllable parameters can be listed as the blast design and the explosive characteristics. In addition, the uncontrollable parameters are defined as the rock characteristics properties, which depend on the quarry site, besides the geological structures of the medium. The effect of these previous parameters on *PPV* has been determined by regression analysis. For instance, Nicholls et al.[7] studied the effect of delay time, charge weight, delay interval, overburden, geology and direction of propagation. Moreover, Wiss et al.[8] investigated the effect of local geology, lithology and rock characteristics.

Ranjan et al.[9] show that the rock properties (unit weight, uniaxial compressive strength, rock quality designation and geological strength index) affect the blast wave propagation extensively. They developed a *PPV* prediction model, which includes these important engineering rock properties. Furthermore, the effects of different rock properties were investigated by Nateghi et al.[10] to predict with accuracy the *PPV* models. They found that the particle velocity is less sensitive to change by the geological conditions despite the acceleration or displacement. Hence, these authors concluded that the *PPV* models are consistent and reliable to make predictions.

Recently, several authors have studied the effects of rock joints on the propagation of stress wave, such as peak value attenuation, spectrum and spatial variations. For example, Hao et al.[11] showed that a rock mass usually contains various joints with different aperture widths, and a blast-induced shock wave is characterized by various frequency spectrum. Rock joints act as a series of connected low-pass filters when the wave propagates through a jointed rock mass. Indeed, the high-frequency signals with wave lengths that are shorter than the joint widths are filtered, while the low-frequency signals are allowed to pass with small modifications in the magnitude. Accordingly, the amplitude and frequency of the wave decrease. The orientation of the joints regarding the wave-propagation direction is another important factor. Theoretically, the transmission and reflection of the wave on a joint surface are closely related to its incident angle. [11] These authors showed that the transmission decreases with the increase of the incident angle, whereas the reflection increases.

King et al.[12] measured the magnitudes and durations of high-frequency seismic waves prop- agated in parallel and perpendicular to columnar joints in basalt. They reached lower *PPV* and greater high-frequency attenuation in the perpendicular direction to the joints rather than in the parallel direction.

Further, several researchers have attempted to predict the ground vibrations using an Artificial Neural Network *(ANN)*, which incorporates large number of parameters [13]. These approaches take into account borehole diameter, number of boreholes, borehole length, burden, spacing, stem- ming, charge per delay, horizontal and radial distance to predict *PPV* and frequency. The main disadvantage of *ANN*, that we reproof, is that it works as a black box (hidden layers) without any physical aspect of the considered phenomena.[14]

Other authors attempt to model *BIGV* by using the Finite Element Method *(FEM)*.[15] This type of modelling is

confronted with the complexity of the site (heterogeneity, anisotropy, topography, discontinuities, etc.), which makes the site assessment very difficult.

The potential damage of ground vibrations is largely quantified either in terms of *PPV* and its associated frequency. Based on the resonance phenomena, if the structure is subjected to ground vibrations' waves with frequencies slightly equal to its fundamental frequency, then the vibrations are amplified.[16] However, the structure is going to vibrate at a magnitude, which is less than or equal to the magnitude of ground vibrations, taking into account the case where the frequency of the ground vibration is below the fundamental frequency of the structure. If the frequency of the ground vibration is 40% higher than the fundamental frequency of the structure, thus, it is going to vibrate with lower amplitude than the ground. Moreover, for ground vibration with a predominant frequency, that is doubling the fundamental frequency of the structure; hence, the response will be only 10% of the magnitude vibration at the natural frequency.[17,18]

Siskind et al.[19] investigated the structure response and damage resulting from *BIGV*. They developed a chart for safe blasting considering *PPV* and frequency, known as *USBM* standards. Other standards, slightly different from *USBM* criteria, are available in the literature as the British standard BS 7385[20] and German standard *DIN 4150*.[21]

1.3 Aim of the research

This paper aims to establish the site-specific attenuation law for ground vibration, and to predict the charge's weight per delay (Q) that could be used without affecting the safety of nearby structures (*"Conveyor belt"* and *"Panel 1 (Upper exploitation level)"* sites). Thus, the assessed safe charges are used to design the blasting patterns with suitable delay intervals, in order to enhance the explosive energy, which is used to destroy the rock. The following steps were considered in the present analysis:

– Thirteen trial blasts (signature boreholes *T B*1 to *T B*13) with different charge weight per delay (Q) were performed at the actual excavation site (Tab. 4). Subsequently, the ground vibration data were recorded at different distances (R) using three component engineering seismographs (Fig. 2(a)). Therefore, they were analyzed in terms of *PPV* and its predominant frequency of the ground vibration.
– The achieved vibration data were analyzed by the least square regression method [22] to develop the

empirical relationship between the scaled distance *(SD)* and *PPV*.
– The production blasts (*P B*1 to *P B*3) are then studied, in order to evaluate the accuracy of the achieved law, which provides the *BIGV*.
– Based on this current analysis, site-specific safety criteria were established by using the safety criteria (*USBM* standards).[19]
– The safe charge weights per delay (Q) has been evaluated for *"Conveyor belt"* and *"Panel 1 (Upper exploitation level)"* sites and used to design the blasting patterns.

2 Empirical and probabilistic models

The scientific community has carried out several studies to predict the amplitude of *BIGV*. In fact, these studies can be divided into three groups, namely the statistical modelling *(SM)* based on the Scaled Distance *(SD)*,[23] the numerical modelling based on Finite Element Method *(FEM)*,[24] and finally, the metaheuristic modelling using the Artificial Neural Network *(ANN)*.[25]

Regarding the SM modelling, the first accepted empirical correlation that has been used to evaluate the blast vibrations was developed by Koch et al.[26] It is based on the systematic measurements of *PPV* and its dependence on the distance from the geophones to the blasting Point, as shown in Eq. 1.

$$PPV = kQ^b R^{-m} \qquad (1)$$

where *PPV* is the peak particle velocity. *k*, *b* and *m* are empirical factors, which may vary according to the geological and geomechanical conditions, besides the applied drilling, blasting and ignition techniques. Q is the charge weight per delay and R is the distance between the blasting and the measurement point.

Eq. 1 was slightly modified by *USBM* (US Mines Office),[25] as expressed in Eq. 2. The Scaled Distance *(SD)* is defined as shown in Eq. 3.

$$PPV = k(SD)^{-\beta} \qquad (2)$$

$$SD = \frac{R}{Q^\alpha} \qquad (3)$$

Figure 1: Location of the Bargny site.

where α is the explosive power ($\frac{1}{2}$ for spherical blast and $\frac{1}{3}$ for cylindrical blast). In addition, k and β represent specific site parameters.

Other empirical equations have been suggested by different researchers to describe the attenuation of blast vibrations, such as Dowding et al.,[27] Duvall et al.,[28] Ghosh et al.,[29] Gupta et al.[30] and Roy et al.[31] However, Koch's fundamental finding[26] of the considerable effect of the charge weight and the distance on the vibrations is still widely accepted. Recently, many authors used Eq. 2 and compared it with the measured *PPV*, in order to evaluate the charge weight per delay.[32,33] A summary of the various *PPV* models is presented in Tab. 1.

The equations reported in Tab. 1 are mainly based on statistical analysis. The field experiments have to be carried out to determine the site parameters using the linear regression analysis. The equations indicate that the *PPV* increases due to the increase of the charge weight per delay (Q) and the decrease of the distance to the blasting. Obviously, the distance from the blasting to the measurement point (R) has a more important effect on *PPV* than the charge per delay (Q).

3 Experimental investigations

3.1 Site description

The site of *"Sococim"* is located in *Senegal*, some thirty kilometers from *Dakar*. It is situated between two villages, the commune of *"Bargny"* in the North West and the commune of *"Rufisque"* in the South Fig. 1. On the *"Rufisque"* side, the *"Gouye Mouride"* district is located at the limit of the factory, more than a kilometer from the quarry. This workers' city is built on blue marls and limestone. On the *Bargny* side, the city of *"Sococim"* is located. *"Sococim"* is relatively close to the blasts when they are located on Panel 1 (about 600 meters). This city is built on the layer of yellow limestone.

The site of *"Bargny"* consists of four lithological units that are described from the bottom to the top as follows:

– in depth, a homogeneous gray limestone, formed by multi-levels with thicknesses ranging from 30 to 60 cm approximately
– a yellow limestone, which contains silex, with 10 to 20 meters of thickness

Figure 2: (a) Vibration monitoring sensor; (b) ANFO truck loader; (c) Blast area inspection; (d) Bottom charge with cartridges and electric detonators.

Table 1: Summary of various *PPV* models.

| N°	References	Empirical models	N°	References	Empirical models
1	Duvall et al. [28]	$V_{ppv} = k \left(\dfrac{R}{\sqrt{W}} \right)^{-b}$	7	Roy et al. [34]	$V_{ppv} = n + k \left(\dfrac{R}{\sqrt{W}} \right)^{-1}$
2	Langefors et al. [35]	$V_{ppv} = k \left(\dfrac{W}{R^{\frac{2}{3}}} \right)^{\frac{b}{2}}$	8	Murmu et al. [36]	$V_{ppv} = k \left(\dfrac{R}{\sqrt{Q}} \right)^{-b} \beta^{\gamma}$
3	Ambraseys et al. [37]	$V_{ppv} = k \left(\dfrac{R}{\sqrt[3]{W}} \right)^{-b}$	9	Rai et al. [38]	$V_{ppv} = kR^{-b}W^a e^{-\alpha R}$
4	IS: 6922 [39]	$V_{ppv} = k \left(\dfrac{R^{\frac{2}{3}}}{\sqrt{W}} \right)^{-b}$	10	Ak et al. [40]	$V_{ppv} = k \left(\dfrac{R}{\sqrt{W}} \right)^{-b} \lambda^{\alpha}$
5	Ghosh et al. [41]	$V_{ppv} = k \left(\dfrac{R}{\sqrt{W}} \right)^{-b} e^{-\alpha R}$	11	Simangunsong et al. [42]	$V_{ppv} = k \left((1 + \cos(\theta_i) + N_c) \dfrac{R}{\sqrt{Q}} \right)^{-b}$
6	Ghosh et al. [41]	$V_{ppv} = k \left(\dfrac{R}{\sqrt[3]{W}} \right)^{-b} e^{-\alpha R}$	12	Kumar et al. [9]	$V_{ppv} = \dfrac{f_c^{0.642} D^{-1.463}}{\gamma}$
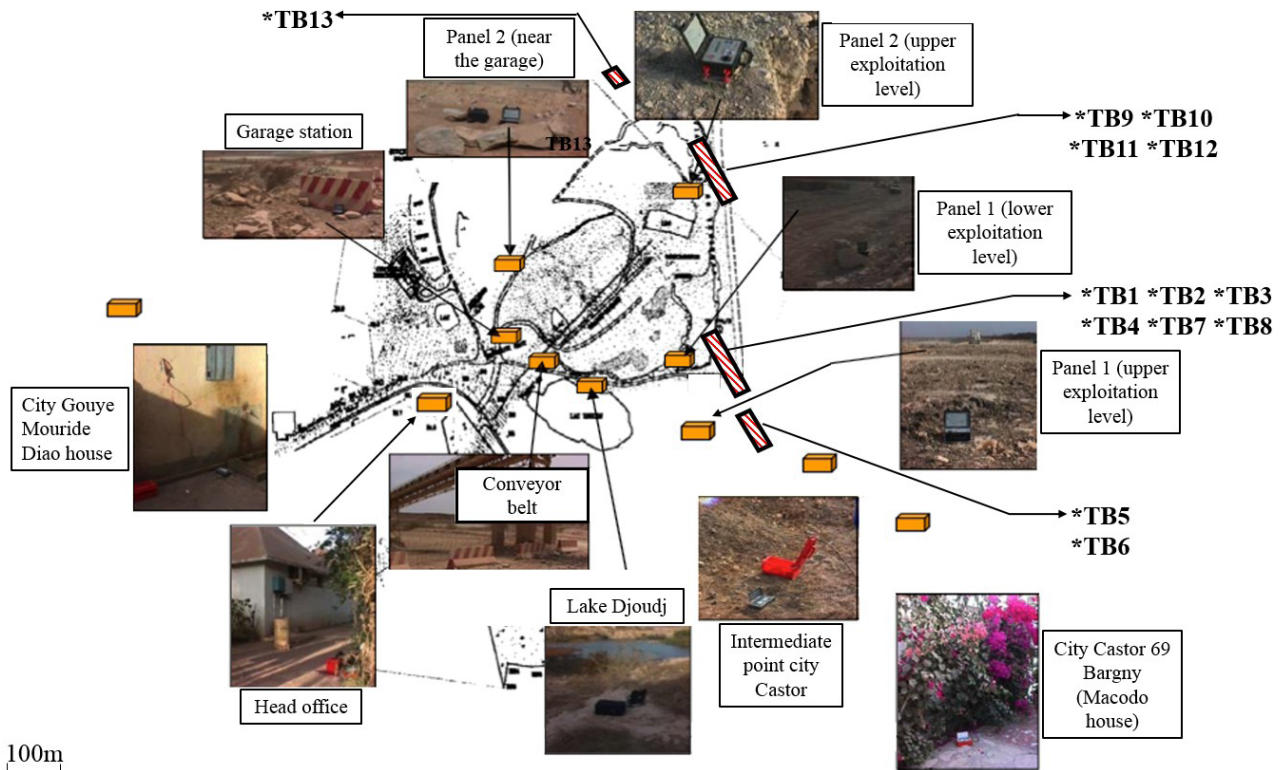
Figure 3: Blast's location and the assessed measurement points.

Table 2: Calculated theoretical specifications[44].

Physical properties	Dynaroc 6 A	Nitram 9	ANFO
Gas volume (0°C/1At) (L/kg)	893	857	898
Total mass energy (MJ/kg)	4.5	4.2	4.6
Total volume energy (MJ/L)	6.4	5	3.7
Detonation pressure (confined) (φ 80 mm) (Gpa)	13.6	13.5	6.9
Detonation temperature (°C)	-	2227	2830
Velocity of detonation (m/s)	-	6200	5200

– an alternation of limestone and marls. This level ensures the transition between the aforementioned limestone level and the surface marl level

– finally, on the surface, a level of marls presenting some beds of limestone that are decreasing toward the east until disappearing

3.2 Technical characteristics of the blasts

The blasts were made using 105, 115 and 165 mm diameter drill boreholes with a depth varying between 7.5 m and 11 m. The boreholes corresponding to the trial blasts *(TB)* were charged with *"Dynaroc 6 90/3150"* and *"Nitram TX9 130/5000"* (Tab. 2). The boreholes corresponding to the production blasts *(PB)* were charged with *"Nitram TX9 130/5000"* and *"ANFO"* elaborated on the quarry site (Tab. 2). Electrical delay detonators were located at the bottom of the boreholes in order to initiate the blasts. The charge weights per delay (Q), for the *TB* experiment, varied from 15 kg to 140 kg as presented in Tab. 4. Moreover, *"Mini seis"*, presented in Fig. 2(a), has been used to record the seismic data. The technical characteristics of this device are shown in Tab. 3.[43] The trigger thresholds were set from 0.4 mm/s to 2 mm/s depending on the distance from the detonation point and the unit load of the explosive that is used. In fact, the selection of these threshold values has to allow the detection of weak ground vibrations, without affecting the initiation of data acquisition, which could be caused by the human activities in the surrounding area.

3.3 Seismic measurements

The vibrations were measured on the bedrock at different distances, varying from 57 m to 1429 m. The ground vibrations were recorded in three space directions, that is, the transverse (*VT*), vertical (*VV*) and longitudinal (*VL*)
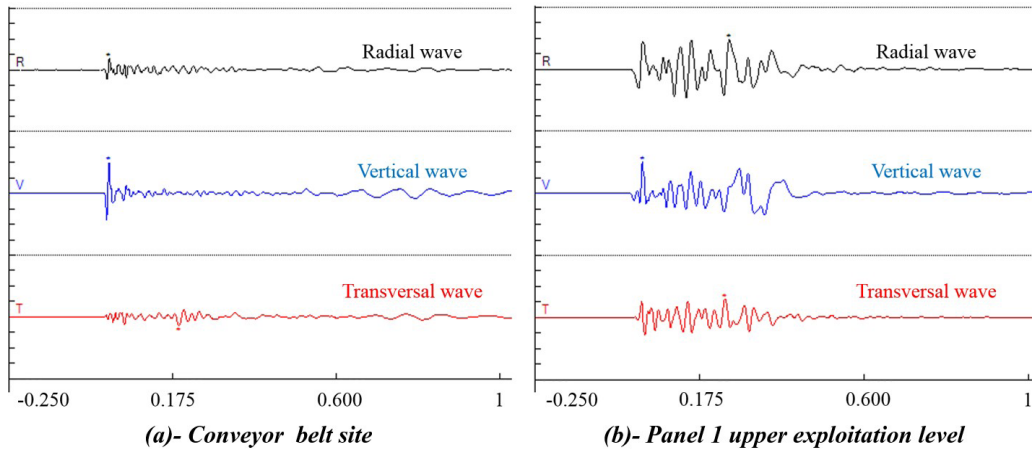
(a)- Conveyor belt site   **(b)- Panel 1 upper exploitation level**

Figure 4: (a) Signal analysis at *"Conveyor belt"* (charge weight per delay 50 kg – distance from blast 436 m); (b) Signal analysis at *"Panel 1 (Upper exploitation level)"* (charge weight per delay 50 kg – distance from blast 150 m).

Table 3: Technical specifications of *"Mini seis"* measuring device[43].

Acquisition	2048 information/lane/second
Storage	storing records on internal memory
Duration of registration	4 seconds
Triggering seismic acquisition	by exceeding the minimum threshold of the sensors
Tri-directional geophones	4.5 Hertz electronically corrected at 2 Hertz

velocity components. Moreover, the air over-pressure was also recorded. The sensors must be bonded to the assessed support, so that they would vibrate identically, otherwise the measurements are disturbed. The connection with the support can be ensured by different technics, either by bolting or sealing the sensor to the support. In addition, all the sensors must be connected to the same acquisition unit so that they are synchronized. The coordinates of each measurement point and each blast were recorded using a *GPS*. Fig. 3 shows the location of the measurement points.

According to the French Regulation Standard *(FRS)*,[45] the *PPV* is defined as the maximum particle velocity component recorded in one of the space directions. Indeed, according to Dowding et al.,[46] the real peak particle velocity is 5 to 10% greater than the maximum single velocity component. This difference remains acceptable since a mathematical treatment on the signal (high-pass filter) is applied, in order to take into account the harmful effect of the amplitudes at low frequencies.

3.4 Trial blast results

Thirteen trial blasts (signature boreholes $TB1$ to $TB13$) with different charge weight per delay (Q) were performed at the actual excavation site. Thereafter, the ground vibration data were recorded at different distances (R) using three component engineering seismographs (Fig. 2(a)). Hence, they were analyzed in terms of *PPV* and its predominant frequency of the ground vibration. The trial blast experiments (from $TB1$ to $TB13$) and the recording of data in terms of the velocity components and the maximal velocity are presented in Tab. 4. The measuring points are listed as follows: *DG*, *P1 (Lower exploitation level)*, *P1 (Upper exploitation level)*, *Lake Ddoudj*, *Macodo's house*, *"Conveyor belt"*, *Garage station*, *Diao's house* and *P2 (Upper exploitation level)* sites.

4 Results and discussion

4.1 Vibration threshold assessment at "Conveyor belt" and "Panel 1 (Upper exploitation level)"sites

Let us consider that the locations to protect from the harmful vibration are respectively the *"Conveyor belt"* and the *"Panel 1 (Upper exploitation level)"* sites presented in Fig. 3, Tab. 4. It should be noted that the railway is located at the *"upper exploitation level"* site; hence, measuring the vibrations has to be carried out using the sensors. Figs. 4(a), 4(b) present the seismic recording wave at the *"Conveyor belt"* and *"Panel 1 (Upper exploitation level)"*

Table 4: Trial blast experiments (from $TB1$ to $TB13$) and the recording of data (velocity components and maximal velocity).

Trial blast (N°)	Measuring points	Measurement distance (m)	Maximal charge per delay (kg)	Sensor ID	Velocities (mm/s)			Maximal velocity (mm/s)
					Longitudinal	Vertical	Transversal	
1	DG	606	15	653	1.4	2.47	0.82	2.47
	P1 (Lower exploitation level)	84	15	2022	15.94	31.82	23.5	31.82
	P1 (Upper exploitation level)	143	15	139	7	8.76	4.7	8.76
	Lake Ddoudj	291	15	2020	8	10.54	7.43	10.54
	Macodo	529	15	1318	2.67	2.8	1.01	2.8
2	DG	613	30	653	1.71	4.12	1.27	4.12
	P1 (Upper exploitation level)	136	30	139	11.05	13.84	7.62	13.84
	P1 (Lower exploitation level)	92	30	2022	20.32	37.72	39.88	39.88
	Lake Ddoudj	297	30	2020	9.46	15.55	12.44	15.55
	Macodo	524	30	1318	4.19	4.57	1.38	4.57
3	DG	634	45	653	1.78	3.56	1.14	3.56
	P1 (Upper exploitation level)	143	45	139	11.18	11.68	8.26	11.68
	P1 (Lower exploitation level)	110	45	2022	20.9	22.1	24.7	24.7
	Lake Ddoudj	320	45	2020	7.62	17.08	14.92	17.08
	Macodo	538	45	1318	5.71	5.33	2.54	5.71
4	DG	582	45	653	0.5	1.01	0.7	1.01
	P1 (Upper exploitation level)	174	45	139	8.64	8.25	6.73	8.64
	P1 (Lower exploitation level)	58	45	2022	10.73	40.45	25	40.45
	Lake Ddoudj	271	45	2020	3.89	5.71	2.98	5.71
	Macodo	555	45	1318	1.52	2.16	1.4	2.16
5	Conveyor belt	469	100	653	2.48	6.98	2.35	6.98
	P1 (Upper exploitation level)	77	100	139	42.67	25.91	25.91	42.67
	Garage station	636	100	2022	2.54	4.32	2.1	4.32
	Lake Ddoudj	302	100	2020	5.78	10.86	8.13	10.86
	Macodo	406	100	1318	6.86	9.27	2.54	9.27

Continued Table 4: Trial blast experiments (from *T B*1 to *T B*13) and the recording of data (velocity components and maximal velocity).

Trial blast (N°)	Measuring points	Measurement distance (m)	Maximal charge per delay (kg)	Sensor ID	Velocities (mm/s)			Maximal velocity (mm/s)
					Longitudinal	Vertical	Transversal	
6	Conveyor belt	458	140	653	2.16	6.35	2.41	6.35
	P1 (Upper exploitation level)	82	140	139	48.26	39.62	25.4	48.26
	Garage station	624	140	2022	2.03	3	1.71	3
	Lake Ddoudj	300	140	2020	5.33	8.76	5.9	8.76
	Macodo	455	140	1318	6.1	8.54	3.43	8.54
7	Conveyor belt	436	50	653	5.34	13.97	3.87	13.97
	P1 (Upper exploitation level)	150	50	139	13	13.84	8.25	13.84
	Garage station	597	50	2022	4.76	7.89	2.98	7.89
	P1 (Upper exploitation level)	89	50	2020	50.1	42.42	35.43	50.1
	Macodo	540	50	1318	8.25	7.49	2.79	8.25
8	Conveyor belt	446	75	653	4.06	11.94	3.81	11.94
	P1 (Upper exploitation level)	138	75	139	13.2	17.8	8.25	17.8
	Garage station	607	75	2022	3.36	5.9	2.41	5.9
	P1 (Lower exploitation level)	98	75	2020	52.96	54.04	23.05	54.04
	Macodo	529	75	1318	7.87	8	2.54	8
9	P2 (Upper exploitation level)	57	15.5	2022	47.56	61.98	27.87	61.98
	P1 (Upper exploitation level)	634	15.5	139	1.27	0.89	1.4	1.4
	Garage station	495	15.5	2020	8.06	7.37	5.33	8.06
	Macodo	1034	15.5	1318	0.51	0.76	0.13	0.76
10	P2 (Upper exploitation level)	64	31	2022	125.2	86.36	33.33	125.22
	P1 (Upper exploitation level)	621	31	139	1.52	1.14	2.16	2.16
	Garage station	500	31	2020	8.13	7.5	5.9	8.13
	Macodo	1020	31	1318	0.89	1	0.25	1

Continued **Table 4:** Trial blast experiments (from *T B*1 to *T B*13) and the recording of data (velocity components and maximal velocity).

Trial blast (N°)	Measuring points	Measurement distance (m)	Maximal charge per delay (kg)	Sensor ID	Velocities (mm/s)			Maximal velocity (mm/s)
					Longitudinal	Vertical	Transversal	
11	Diao	1429	47	653	0.38	0.57	0.25	0.57
	P2 (Upper exploitation level)	76	47	2022	125.4	112.7	37.46	125.41
	Garage station	511	47	2020	9.08	9.65	7.4	9.65
	Macodo	1017	47	1318	1.65	1.9	0.51	1.9
	P1 (Upper exploitation level)	618	47	139	2.67	2.28	3.81	3.81
12	Diao	1422	63	653	0.38	0.7	0.25	0.7
	P2 (Upper exploitation level)	70	63	2022	126.6	105.5	32.51	126.55
	Garage station	507	63	2020	8.95	8.82	7.11	8.95
	Macodo	1025	63	1318	1.9	2.03	0.51	2.03
	P1 (Upper exploitation level)	626	63	139	2.67	2.41	4.06	4.06
13	Diao	1379	44.1	653	0.25	0.44	0.19	0.44
	P2 (Upper exploitation level)	198	44.1	2022	28.19	12.32	17.8	28.19
	Garage station	555	44.1	2020	2.85	2.79	2.54	2.85

sites. As illustrated by the previous figures, the presented curves are characterized by low frequencies that are less than or equal to 10 Hz. However, the recorded magnitudes that correspond to the low frequencies at *"Panel 1 (Upper exploitation level)"* site are important. This result can be explained by the dominance of surface waves.[19]

These types of signals are often associated with a geological environment that includes intercalation of geological layers with low thickness (10 to 20 m) and different mechanical characteristics.[47] It is indeed, the case of the considered site of *"Sococim"*, which is characterized by the intercalation of marls and massive limestone.

The maximum velocities in each direction and their associated pseudo frequencies for the previous sites to protect are presented in Fig. 5 in conjunction with the *USBM RI 8507* criterion.[19] The pseudo frequency analysis method is based on the elapsed time and the maximum velocity observed with two successive intersections with the x-axis that refers to the time evolution. Therefore, the dominant frequency is defined as the inverse of twice of this elapsed time. The frequency-based safe vibration

limits for cosmetic cracks were established for *"Conveyor belt"* and *"Panel 1 (Upper exploitation level)"* sites, as it is presented in Figs. 5(a) and 5(b). The *USBM RI 8507* criterion[19] has the following displacement and velocity values for the four ranges of the dominant frequency,[48] namely, 0.76 mm for 1–4 Hz, 19 mm/s for 4–13.7 Hz, 0.2 mm for 13.7–40 Hz, and 50.8 mm/s for 40–100 Hz. In addition, a limit of 19 mm/s for 4–13.7 Hz is used for drywall, while the limit of 12.7 mm/s for 2.5–10 Hz is applied for plaster. The frequency zones below 4 Hz and above 40 Hz are still not well defined according to Dowding et al.[46] In fact, the relation between *PPV*, the frequency and these zones are currently the subject of advanced research. It is noted that the *PPV* values for a given frequency remain below the thresholds established by this criterion. For the pseudo frequencies measured at the *"Conveyor belt"* and *"Panel 1 (Upper exploitation level)"* sites, the *PPV* threshold should be fixed according to the *USBM RI 8507*.[19]

However, a complete analysis of the signal for each measuring point, in particular with the Fast Fourier Transform *(FFT)*, is necessary to get further information.
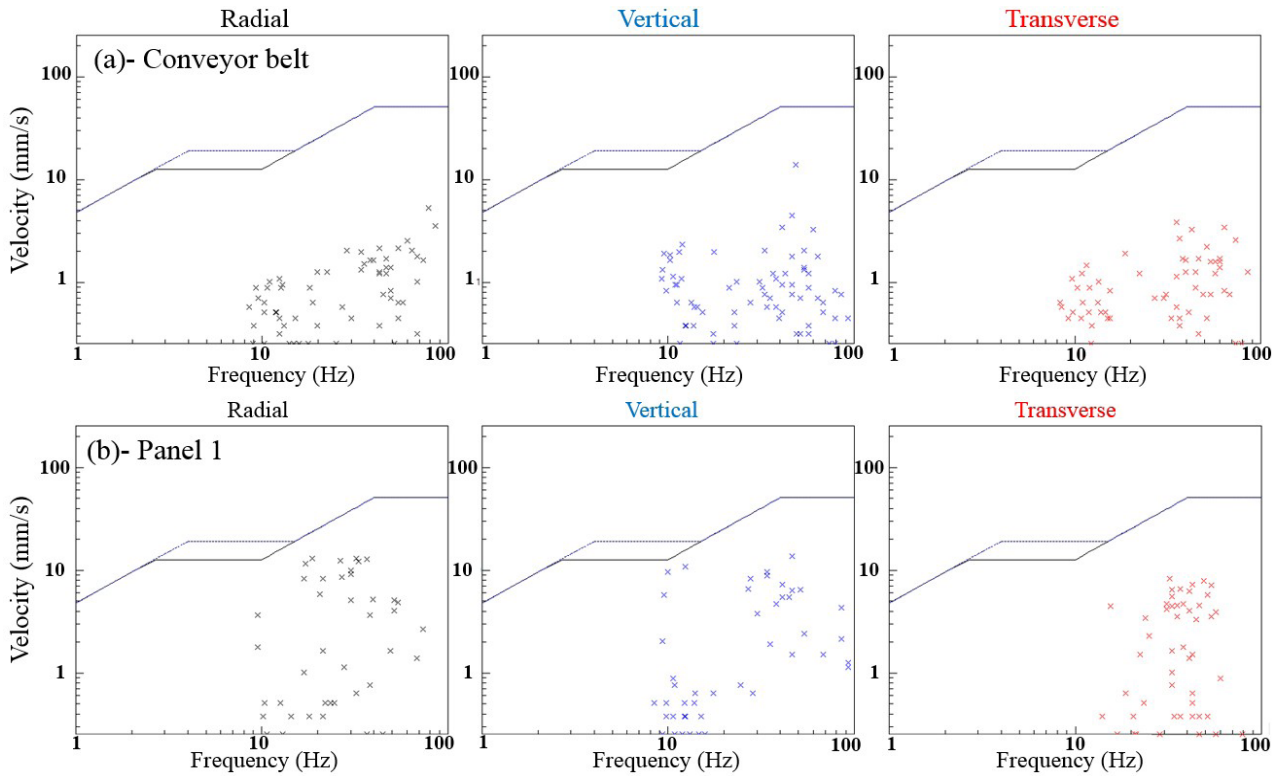
Figure 5: *PPV* and its associated frequencies with *USBM RI 8507* criterion. (a) *"Conveyor belt" site*, (b) *"Panel 1 (Upper exploitation level)" site*.
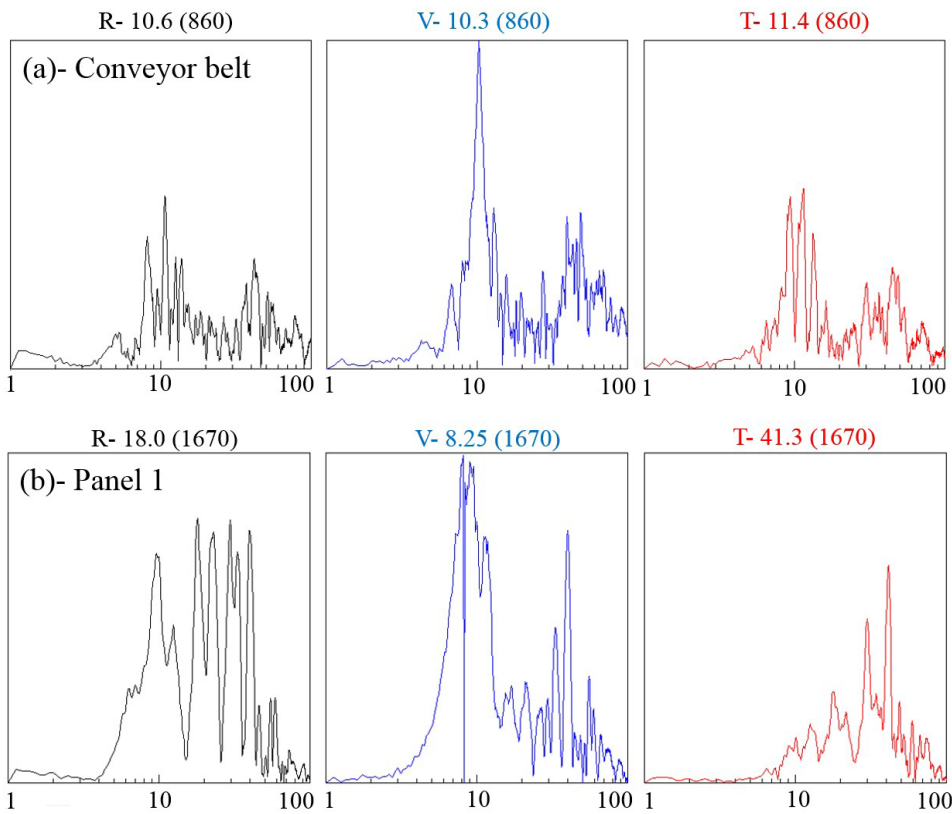

Figure 6: Fast Fourier Transform (FFT) analysis of the vibration signal at (a) "Conveyor belt" site and (b) *"Panel 1 (Upper exploitation level)"*.
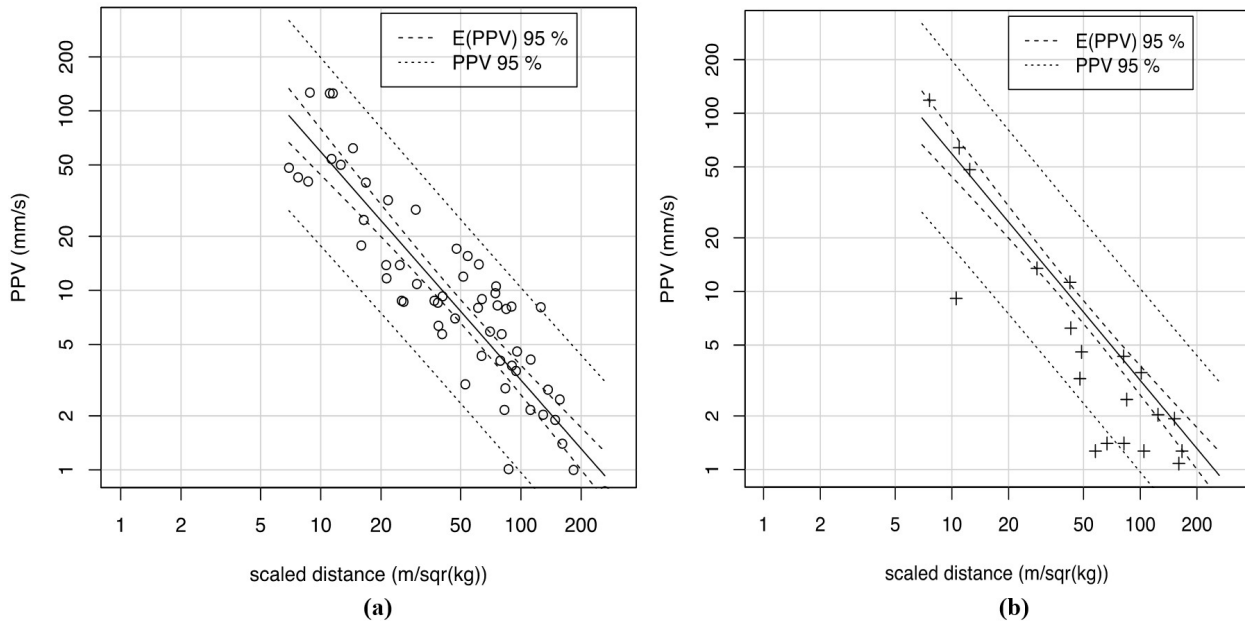

Figure 7: (a) Least squares regression and 95% confidence level curves with the used trial blasts; (b) Observed production blasts and 95% confidence level curves.

[49] *FFT* analysis confirms these observations by showing peaks at low frequencies, which are less than 10 Hz (Fig. 6). Therefore, this frequency analysis is necessary in order to predict and assess the nature of vibrations and their harmful effect on the surrounding structures.

4.2 Attenuation law of the blast vibration

The attenuation of blast vibration is commonly studied empirically using the field data collected by trial detonations. In this study, thirteen trial blasts (TB) located at the actual excavation site previously presented in Fig. 1 are used. The relation between the charge weight (Q), the distance (R) and the *PPV* amplitude forms the basis of the attenuation relation. As cited before, Eq. 2 is the most used model for predicting the attenuation of ground vibrations with accuracy. The trial blasts *(TB)* were made using 165 mm diameter drill boreholes with 11 m of length. The charge weights per delay (Q) varied from 15 kg to 140 kg. The vibrations were measured at different distances varying from 57 m to 1429 m.

The ground vibration data pairs, the scaled distance *SD* and the *PPV*, were plotted on log-log scale as shown in Fig. 7(a). The least square regression analysis method was used to determine the site constants k and β expressed in Eq. 2. The mean and the 95% confidence level attenuation
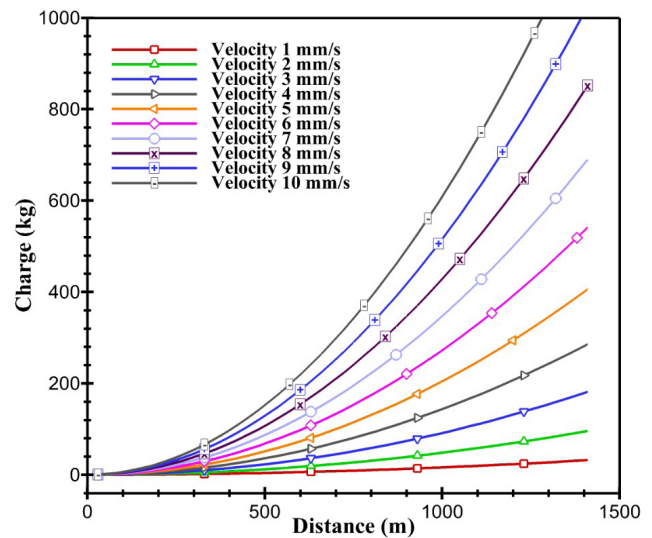

Figure 8: Safe charge weight per delay (Q) for different distances and velocities.

laws obtained from the regression analysis of the data are written as expressed in Eqs. 4, 5.[22]

$$PPV = 1101 \left(\frac{R}{\sqrt{Q}} \right)^{-1.27} \qquad (4)$$

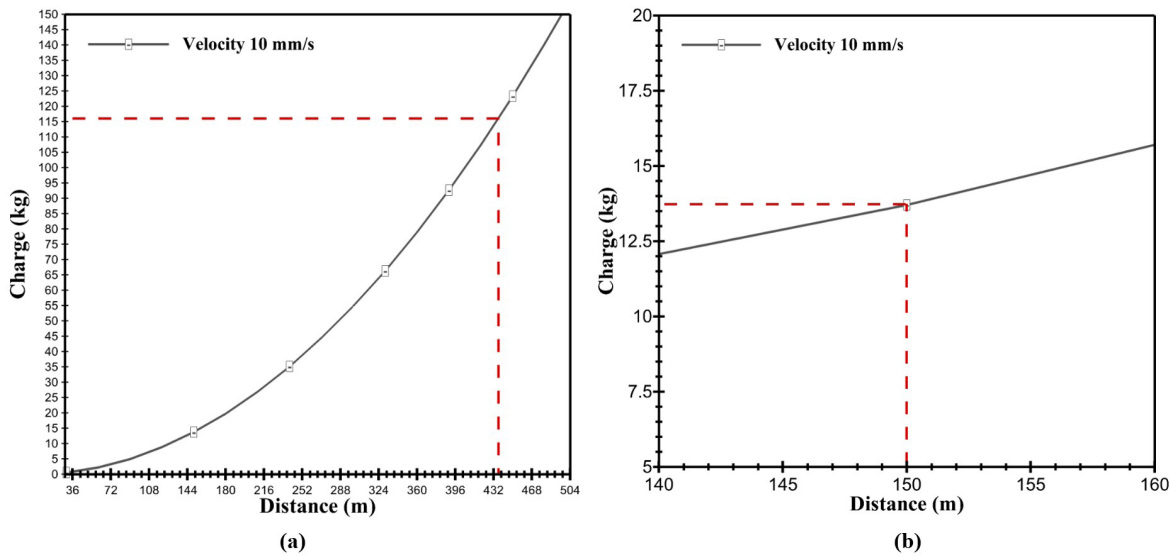$$PPV = 3539 \left(\frac{R}{\sqrt{Q}} \right)^{-1.27} \qquad (5)$$

Figure 9: (a) Safe charge weight per delay (Q) for *"Conveyor belt"* site; (b) Safe charge weight per delay for *"Panel1 (Upper exploitation level)"* site.

The production blasts *T P*1 to *T P*3, which were not used to determine the site parameters k and *β*, are shown in Fig. 7(b). It should be noted that all the points are nearly within the confidence interval established from trial blasts (Tab. 4). Our prediction, from this point of view, is acceptable and the law previously validated would provide with accuracy of the *BIGV*.

The trial blasts that have been carried out in *"Sococcim quarry"* are entirely confined, while the production blasts have a free face. The energy transmitted to the rock is increased with increasing the burden, which leads to higher vibration levels.[50,51] In the present case, the trial blasts have an "infinite burden" (without a free face). This explains the fact that PPVs obtained for the production blasts tend to be a little bit smaller (by an average) in comparison with the regression line obtained from the trial blasts results.

4.3 Assessment of safe charge weights per delay (Q)

The safe vibration levels were used with the site-specific attenuation relation (Eq. 2), to assess and predict the safe charges per delay (Q). Indeed, the safe charges weight per delay are presented in Fig. 8, they were achieved for distances varying from 58 m to 1422 m and for velocities varying from 1 to 10 mm/s. The safe weight charge per delay (Q) for the *"Conveyor belt"* site is 116 kg (Fig. 9(a)), while the safe weight charge per delay (Q) for the *"Panel 1 (Upper exploitation level)"* site is 13.75 kg (Fig. 9(b)).

The weight charge per delay (Q) of 50 kg can be considered as a safe charge weight for *"Panel 1 (Upper exploitation level)"* site, which is located at 150 m from the nearest blast, because it satisfies the *USBM RI 8507* criterion[19] (Fig. 5(b)). However, as previously discussed from Figs. 4(b) and 6(b), the presence of low frequencies with amplitudes similar to those recorded for high frequencies would impose the use of an optimized weight charge per delay (Q) (13.75 kg as shown in Fig. 9(b)), in order to not exceed the threshold of 10 mm/s for the frequencies slightly below 10 Hz.

4.4 Blasting pattern design and optimization

The iso-velocity maps presented in Fig. 8 showed the importance of selecting with accuracy the charge weight per delay (Q), in order to meet a comfort threshold of 10 mm/s, and to enhance the productivity requirements from the quarry site. The limitation of the charge weight per delay requires the use of several solutions:

– The use of multi-detonation in the case of small applied charges
– The use of boreholes' diameters of 105 to 165 mm, with a single detonation

According to the distance between the blast and the nearest sites, namely, the *"Conveyor belt"* site and the *"Panel 1 (Upper exploitation level)"* site, the attenuation equation of blast vibration imposes the use of charge weight per delay of 116 kg and 13.75 kg respectively.
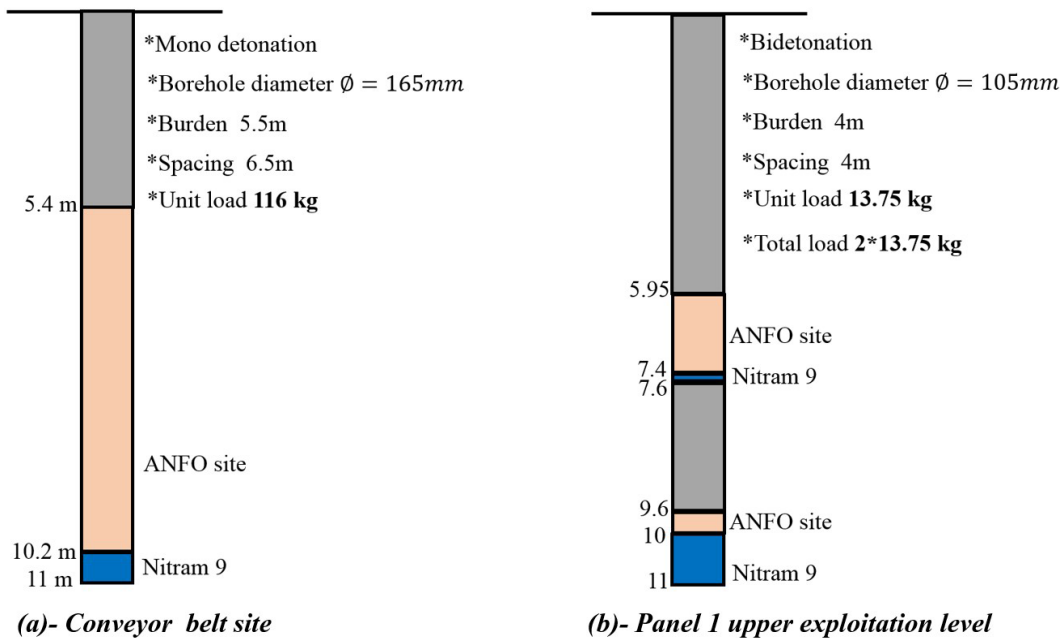
(a)- Conveyor belt site

(b)- Panel 1 upper exploitation level

Figure 10: The blast design of charge structure in different site: (a) *"Conveyor belt"* site; (b) *"Panel 1 (Upper exploitation level)"* site.

4.4.1 "Conveyor belt" site

A charge weight per delay of 116 kg can be conceived by using the following blast design, which is presented in Fig. 10(a) for the *"Conveyor belt"* site.

4.4.2 "Panel 1 (Upper exploitation level)" site

A charge weight per delay of 13.75 kg can be conceived by using the following blast design, which is presented in Fig. 10(b) for the *"Panel 1 (Upper exploitation level)"* site.

5 Conclusion

This paper proposes a generalized methodology of blasting that helps to ensure the comfort of the inhabitants and the safety of structures against damage, which is induced by blast vibrations. The site-specific attenuation relation developed from ground vibration data observed from trial blasts *(TB)* is used for predicting the *PPV* at different distances and with different charge weights. The production blasts *(PB)*, which were not used to determine the site-specific attenuation, were analyzed to confirm the relevance of the adopted model. Subsequently, the *USBM RI 8507* criterion was used to validate that the measured velocities associated with their pseudo frequencies do not exceed the allowed thresholds.

This analysis remains insufficient. Indeed, the signal processing by FFT can highlight the low frequencies' predominance, which characterizes the surface wave phenomena. Although the vibration levels measured at these points are low (always less than 10 mm/s), this phenomenon can be felt as an *"earthquake"* due to the resonance effect. Finally, the attenuation model has been used to evaluate the safe charge weights of the explosive (Q) to be used at the *"Conveyor belt"* site and at the *"Panel 1 (Upper exploitation level)"* site. The safe charge weights per delay (Q) were respectively 116 kg and 13.75 kg.

References

[1]   L. Ma, Z. Li, J. Liu, L. Duan, J. Wu, Mechanical properties of coral concrete subjected to uniaxial dynamic compression, Construction and Building Materials 199 (2019) 244 – 255. doi:https://doi.org/10.1016/j. conbuildmat.2018.12.032. URL http://www.sciencedirect.com/science/article/pii/ S0950061818330125

[2] H. Agrawal, A. Mishra, Probabilistic analysis on scattering effect of initiation systems and concept of modified charge per delay for prediction of blast induced ground vibrations, Measurement 130 (2018) 306–317. doi: https://doi.org/10.1016/j.measurement.2018.08.032. URL http://www.sciencedirect.com/science/article/pii/S0263224118307759

[3] B. Duan, H. Xia, X. Yang, Impacts of bench blasting vibration on the stability of the surrounding rock masses of roadways, Tunneling and Underground Space Technology 71 (2018) 605–622. doi:https://doi.org/10.1016/j.tust.2017.10.012. URL http://www.sciencedirect.com/science/article/pii/S0886779817303371

[4] C. E. Anderson Jr, T. Behner, C. E. Weiss, Mine blast loading experiments, International Journal of Impact Engineering 38 (8-9) (2011) 697–706.

[5] T. Ngo, P. Mendis, A. Gupta, J. Ramsay, Blast loading and blast effects on structures–an overview, Electronic Journal of Structural Engineering 7 (S1) (2007) 76–91.

[6] M. Monjezi, M. Hasanipanah, M. Khandelwal, Evaluation and prediction of blast-induced ground vibration at shur river dam, iran, by artificial neural network, Neural Computing and Applications 22 (7-8) (2013) 1637–1643.

[7] H. R. Nicholls, C. F. Johnson, W. I. Duvall, Blasting vibrations and their effects on structures, US Government Printers, 1971.

[8] J. F. Wiss, Control of vibration and blast noise from surface coal mining, Bureau of Mines, Open File Rept.

[9] R. Kumar, D. Choudhury, K. Bhargava, Determination of blast-induced ground vibration equations for rocks using mechanical and geological properties, Journal of Rock Mechanics and Geotechnical Engineering 8 (3) (2016) 341–349.

[10] R. Nateghi, Prediction of ground vibration level induced by blasting at different rock units, International Journal of Rock Mechanics and Mining Sciences 48 (6) (2011) 899–908.

[11] H. Hao, Y. Wu, G. Ma, Y. Zhou, Characteristics of surface ground motions induced by blasts in jointed rock mass, Soil Dynamics and Earthquake Engineering 21 (2) (2001) 85–98.

[12] M. King, L. Myer, J. Rezowalli, Experimental studies of elastic-wave propagation in a columnar-jointed rock mass, Geophysical prospecting 34 (8) (1986) 1185–1199.

[13] M. Khandelwal, T. Singh, Prediction of blast-induced ground vibration using artificial neural network, Interna- tional Journal of Rock Mechanics and Mining Sciences 46 (7) (2009) 1214–1222.

[14] M. Monjezi, M. Ghafurikalajahi, A. Bahrami, Prediction of blast-induced ground vibration using artificial neural networks, Tunnelling and Underground Space Technology 26 (1) (2011) 46–50.

[15] J. Torano, R. Rodriguez, Simulation of the vibrations produced during the rock excavation by different methods, WIT Transactions on Modelling and Simulation 33.

[16] Y. S. Chae, Design of excavation blasts to prevent damage, Civil Engineering 48 (4).

[17] W. I. Duvall, D. E. Fogelson, Review of criteria for estimating damage to residences from blasting vibrations, US Department of the Interior, Bureau of Mines, 1962.

[18] A. T. Edwards, T. Northwood, Experimental studies of the effects of blasting on structures, Division of Building Research, National Research Council, 1960.

[19] U. S. B. of Mines, D. Siskind, Structure response and damage produced by ground vibration from surface mine blasting, US Department of the Interior, Bureau of Mines New York, 1980.

[20] K. Avellan, E. Belopotocanova, M. Puurunen, Measuring, monitoring and prediction of vibration effects in rock masses in near-structure blasting, Procedia engineering 191 (2017) 504–511.

[21] J. Guggenberger, G. Mu¨ller, Erschu¨tterungen, in: Taschenbuch der Technischen Akustik, Springer, 2004, pp. 767–801.

[22] M. Khandelwal, T. Singh, Prediction of blast induced ground vibrations and frequency in opencast mine: a neural network approach, Journal of sound and vibration 289 (4-5) (2006) 711–725.

[23] Y. Zeng, H. Li, X. Xia, B. Liu, H. Zuo, J. Jiang, Blast-induced rock damage control in fangchenggang nuclear power station, china, Journal of Rock Mechanics and Geotechnical Engineering 10 (5) (2018) 914–923.

[24] X. Zhao, G. Wang, W. Lu, M. Chen, P. Yan, C. Zhou, Effects of close proximity underwater explosion on the nonlinear dynamic response of concrete gravity dams with orifices, Engineering Failure Analysis 92 (2018) 566–586.

[25] B. Elevli, E. Arpaz, Evaluation of parameters affected on the blast induced ground vibration (bigv) by using relation diagram method (rdm), Acta Montanistica Slovaca 15 (4) (2010) 261.

[26] H. Koch, Zur m¨oglichkeit der abgrenzung von lademengen bei steinbruchsprengungen nach festgestellten er-schu¨tterungsst¨arken, Nobel Hefte 24 (1958) 92–96.

[27] G. Athanasopoulos, P. Pelekis, Ground vibrations from sheetpile driving in urban environment: measurements, analysis and effects on buildings and occupants, Soil dynamics and earthquake engineering 19 (5) (2000) 371–387.

[28] W. I. Duvall, B. Petkof, Spherical propagation of explosion-generated strain pulses in rock, Tech. rep., Bureau of Mines (1958).

[29] A. Ghosh, J. J. Daemen, Statistics–a key to better blast vibration predictions, in: Proceedings of the 26th US Symposium on Rock Mechanics, Rapid City, 1985, pp. 1141–1149.

[30] R. Gupta, P. P. Roy, B. Singh, On a blast induced blast vibration predictor for efficient blasting, in: Proceedings of the 22nd international conference of safety in Mines, Beijing, China, 1988, pp. 1015–1021.

[31] P. Roy, Putting ground vibration predictions into practice, Colliery Guardian 241 (2) (1993) 63–7.

[32] B. Mu¨ller, J. Hausmann, H. Niedzwiedz, Comparison of different methods of measuring and calculating blast vibrations in rock masses, in: The 4th EFEE World Conference, Vienna, 2007.

[33] M. Monjezi, H. A. Khoshalan, A. Y. Varjani, Prediction of flyrock and backbreak in open pit blasting operation: a neuro-genetic approach, Arabian Journal of Geosciences 5 (3) (2012) 441–448.

[34] P. P. Roy, Vibration control in an opencast mine based on improved blast vibration predictors, Mining Science and Technology 12 (2) (1991) 157–165.

[35] U. Langefors, B. Kihlstrom, The modern techniques of rock blasting. john wiely and sons, Inc, New York, 438pp. [36] S. Murmu, P. Maheshwari, H. K. Verma, Empirical and probabilistic analysis of blast-induced ground vibrations, International Journal of Rock Mechanics and Mining Sciences 103 (2018) 267–274.

[37] N. Ambraseys, A. Hendron, Dynamic behaviour of rock masses, Rock Mechanics in Engineering Practice (1968) 203–207Cited By 118.

[38] R. Rai, T. Singh, A new predictor for ground vibration prediction and its comparison with other predictors, Indian Journal of Engineering and Materials Sciences 11 (3) (2004) 178–184, cited By 30. URL https://www.scopus.com/inward/record.uri?eid=2-s2.0-6344246317&partnerID=40&md5=2aebef919c009924f500c07622f81484

[39] I. Indian Standard, Criteria for safety and design of structures subjected to underground blast, Bulletin No: IS-6922, Bureau of Indian Standards, New Delhi, India.

[40] H. Ak, A. Konuk, The effect of discontinuity frequency on ground vibrations produced from bench blasting: a case study, Soil Dynamics and Earthquake Engineering 28 (9) (2008) 686–694.

[41] A. Ghosh, J. J. Daemen, et al., A simple new blast vibration predictor (based on wave propagation laws), in: The 24th US Symposium on Rock Mechanics (USRMS), American Rock Mechanics Association, 1983.

[42] G. M. Simangunsong, S. Wahyudi, Effect of bedding plane on prediction blast-induced ground vibration in open pit coal mines, International Journal of Rock Mechanics and Mining Sciences (79) (2015) 1–8.

[43] M. Iphar, M. Yavuz, H. Ak, Prediction of ground vibrations resulting from the blasting operations in an open-pit mine by adaptive neuro-fuzzy inference system, Environmental Geology 56 (1) (2008) 97–107.

[44] C. Coulombez, Analyse et optimisation des pratiques d'abattage a l'explosif dans une carri`ere de granulats.

[45] B. Skipp, Ground vibration–codes and standards, Ground dynamics and man-made processes. The Institution of Civil Engineers, United Kingdom (1998) 29–41.

[46] C. H. Dowding, R. D. Hryciw, A laboratory study of blast densification of saturated sand, Journal of Geotechnical Engineering 112 (2) (1986) 187–199.

[47] A. P. J.F. SEMBLAT, Waves and vibrations in soils: Earthquakes, traffic, shocks, construction works.

[48] D. Grothe, P. Reinders, Advanced vibration management in quarries using a predictive blast vibration model, Vienna Confer-ence Proceedings, European Federation of Explosives Engineers, UK (2007) 93–106.

[49] D. Park, B. Jeon, S. Jeon, A numerical study on the screening of blast-induced waves for reducing ground vibration, Rock mechanics and rock engineering 42 (3) (2009) 449–473.

[50] M. Ramulu, A. Raina, A. Chakraborty, A. Reddy, J. Jethwa, Influence of burden on the intensity of ground vibrations in a limestone quarry, in: Proceedings of the International Conference fragmentation and blasting, Fragblast, 2002, pp. 617–624.

[51] T. B. Afeni, S. K. Osasan, Assessment of noise and ground vibration induced during blasting operations in an open pit mine — a case study on Ewekoro limestone quarry, Nigeria, Mining Science and Technology (China) 19 (4) (2009) 420 – 424. doi:https://doi.org/10.1016/S1674-5264(09)60078-8. URL http://www.sciencedirect.com/science/article/pii/S1674526409600788